Measurement of Dipolar Contributions to $^1J_{CH}$ Splittings from Magnetic-Field Dependence of J Modulation in Two-Dimensional NMR Spectra

Nico Tjandra and Ad Bax

Laboratory of Chemical Physics, National Institute of Diabetes and Digestive and Kidney Diseases, National Institutes of Health, Bethesda, Maryland 20892-0520

Anisotropy of the magnetic susceptibility tensor, $\boldsymbol{\chi}$, of a molecule results in an orientation-dependent interaction energy, E, when it is placed in a magnetic field, B_0:

$$E = -B_0 \cdot \boldsymbol{\chi} \cdot B_0 / 2\mu_0. \qquad [1]$$

For monomeric proteins in solution, E is much smaller than kT, and the susceptibility anisotropy results in a very small degree of alignment with the magnetic field. As a consequence, dipolar couplings no longer average to zero but have a small residual value which scales with the square of B_0. The magnitude of the dipolar coupling contains information on the orientation of the internuclear vector relative to the susceptibility tensor and therefore potentially contains valuable structural information. Such dipolar couplings have been observed in a range of small molecules with relatively large magnetic shielding susceptibility anisotropy, such as polycyclic aromatics and porphyrins (*1–4*), and in molecules anchored to discoidal micelle systems (*5, 6*).

Recently, Tolman *et al.* (*7*) have shown that magnetic-field alignment of the paramagnetic protein myoglobin results in a measurable change of the apparent $^1J_{NH}$ splittings, which represents the sum of the true $^1J_{NH}$ coupling and the residual ^{15}N–^1H dipolar coupling. Similarly, Kung *et al.* showed relatively large changes in $^1J_{CH}$ for increasing magnetic-field strengths in a natural-abundance DNA dodecamer (*8*). The magnetic susceptibility anisotropy calculated for the diamagnetic protein ubiquitin is more than an order of magnitude smaller than that of myoglobin or the DNA dodecamer and results in very small changes in $^1J_{NH}$ (≤ 0.25 Hz) when the magnetic-field strength is increased from 8.5 to 14 T (*9*). Nevertheless, both the magnitude and orientation of the susceptibility anisotropy, calculated from the very weak field dependence of the backbone ^{15}N–^1H J splittings, were found to be in good agreement with the susceptibility anisotropy calculated on the basis of ubiquitin's X-ray structure.

Here, we present a method for accurate measurement of the field dependence of $^1J_{CH}$ in proteins uniformly enriched in ^{13}C. We restrict ourselves to CH sites; for CH_2 sites, the

relatively efficient ^1H–^1H spin flips of the methylene protons complicate the measurement. For methyl groups, the rapid rotation around the threefold symmetry axis reduces the dipolar coupling, making accurate quantitative measurement difficult. Application of the new method to ubiquitin indicates that the difference in the $^1J_{C\alpha H\alpha}$ splitting at 360 and 750 MHz ^1H frequencies can be measured with an accuracy of about 0.3 Hz. The method is therefore expected to be useful for measurement of dipolar couplings in systems with a relatively large susceptibility anisotropy, such as protein–DNA complexes (Tjandra *et al.,* unpublished results).

Figure 1 shows the pulse scheme used in the present study, which is a variation on the regular CT-HSQC experiment (*10–12*). By altering the time point at which the ^1H 180° pulse is applied during the constant-time evolution period, the intensity in the correlation spectrum becomes a simple function of $^1J_{CH}$ and permits this coupling to be calculated from the observed intensities (*9, 13*). Pulsed-field-gradient coherence selection is used to maximize suppression of the solvent signal. Note that the experiment is preferably applied in H_2O solution which, because of its lower viscosity relative to D_2O, yields favorable $^{13}C^\alpha$ relaxation times. Unfortunately, when adding the ''Rance–Kay'' sensitivity-enhancement feature to this sequence (*14*), we find that there is a nearly uniform small change in the measured $^1J_{CH}$ values (typically ≤ 2 Hz), which, at least in part, is attributed to pulse imperfection. Therefore, despite its signal-to-noise being up to twofold higher, this Rance–Kay feature is not used in the present study.

Using the scheme of Fig. 1, the intensity of a ^{13}C–^1H correlation in the 2D CT-HSQC spectrum is proportional to $\cos[2\pi\,^1J_{CH}\,(T - \Delta)]$. $^1J_{CH}$ is then determined by optimizing the fit between $C \times \cos[2\pi\,^1J_{CH}\,(T - \Delta)]$ and the intensities observed for different Δ durations. As usual, the duration of $2T$ is adjusted to $1/^1J_{CC} \approx 28$ ms. The value of $^1J_{CH}$ is determined most accurately if the set of acquired spectra includes one or more Δ values for which $\sin[2\pi\,^1J_{CH}\,(T - \Delta)]$ is close to zero, i.e., where the intensity is the steepest function of $^1J_{CH}$. In order to cover a wide range
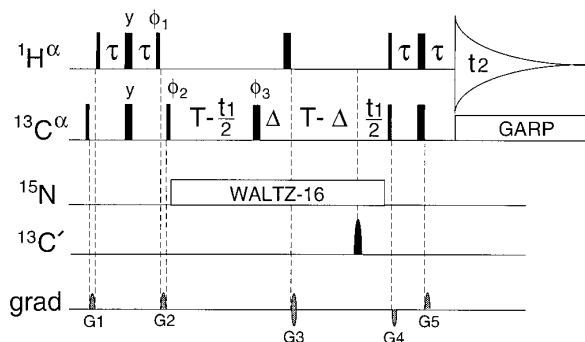
FIG. 1. Pulse scheme of the 2D $^1J_{CH}$-modulated ^{13}C–^1H CT-HSQC experiment. Narrow and wide pulses correspond to 90° and 180° flip angles, respectively, with phase x, unless indicated. The pulse width of the $180_{\phi 2}$ pulse is adjusted to $\sqrt{3}/(2\Delta\delta)$ seconds (where $\Delta\delta$ is the difference in resonance frequency between the ^{13}C carrier and the center of the carbonyl region), such that its excitation profile has a null at the $^{13}C'$ frequency. The $^{13}C'$ 180° pulse is sine-bell shaped and has a duration of $4/\Delta\delta$ seconds. All other pulses are applied at high power. The ^1H 180° pulse applied during the constant-time evolution period is of the composite, $90°_x$ — $180°_y$ — $90°_x$, type. The ^{13}C carrier is positioned at 56 ppm. Delay durations: $\tau = 1.5$ ms; $2T = 28$ ms; $\Delta = 4$ μs – 2.35 ms. Phase cycling: $\phi_1 = y, -y$; $\phi_2 = x, x, y, y, -x, -x, -y, -y$ for positive G_3 gradient; $\phi_2 = x, x, -y, -y, -x, -x, y, y$ for negative G_3 gradient; $\phi_3 = 8(x), 8(y), 8(-x), 8(-y)$; Rec. = $x, -x, y, -y, -x, x, -y, y, -x, x, -y, y, x, -x, y, -y$. All gradients are sine-bell shaped with 25 G/cm at their center. Gradient durations: $G_{1,2,3,4,5} = 1.85, 4.3, 3.93, 0.7, 0.3$ ms. Quadrature in the t_1 dimension is obtained by coherence transfer pathway selection, carefully fine tuning the duration of gradient G_3 in order to maximize magnetization transfer from ^{13}C to ^1H. For each t_1 duration, two FIDs are acquired, one with a positive polarity of G_3, and one with a negative polarity. The sum and difference of this pair of FIDs provide the two components of the t_1 quadrature signal (20, 21).

of $^1J_{CH}$ couplings, we therefore prefer to record a set of spectra with different Δ durations, such that the factor $\sin[2\pi\,^1J_{CH}(T - \Delta)]$ changes sign at the edges of the range of ^1J values to be covered. For $^1J_{C\alpha H\alpha}$ values in the range 134–150 Hz, Δ values ranging from 0.9 to 2.35 ms are used, in addition to a time point for which $\Delta = 0$.

As noted previously (15), relaxation interference (cross correlation) can affect the accuracy of one-bond J coupling measurements. Fortunately, $^{13}C^\alpha$ chemical-shift anisotropy (CSA) is relatively small, and cross correlation between the $^1H^\alpha$–$^{13}C^\alpha$ dipolar and $^{13}C^\alpha$ CSA interactions gives rise to a very weak, dispersive (15) contribution in the ^{13}C dimension of the ^1H–^{13}C CT-HSQC spectrum, which has no significant effect on the measurement of $^1J_{CH}$. However, the effect of dipole–dipole cross correlation can be significant. Consider, for example, a three-spin system, ISX, where I is the H^α spin, S is C^α, and X is an H^N, H^β, or H^γ proton, J-coupled to C^α. At the end of the constant-time evolution period, the four S-spin multiplet components make angles of $\pm 2\pi(J_{IS} \pm J_{XS})(T - \Delta)$ with the y axis (Fig. 2A). As a result of cross correlation between the SI and SX dipolar relaxation mechanisms, the multiplet components corresponding to the same spin state of I and X will relax at a different rate relative to the case where they have opposite spin states

(16). Assuming rigid body isotropic tumbling with a correlation time τ_c and an ISX angle α, the S-spin relaxation rate equals $R_{SI} + R_{SX} \pm R_{CC}$, where R_{SI} and R_{SX} are the S–I and S–X dipolar contributions, and R_{CC} is the interference term, with the "+" sign referring to identical spin states of I and X and the "−" sign referring to opposite spin states. In the slow-tumbling limit, these terms are given by

$$R_{SI} = \tfrac{1}{5}J(0)(\mu_0/4\pi)^2 h^2 \gamma_S^2 \gamma_I^2/(4\pi^2 r_{SI}^6) \qquad [2a]$$

$$R_{SX} = \tfrac{1}{5}J(0)(\mu_0/4\pi)^2 h^2 \gamma_S^2 \gamma_X^2/(4\pi^2 r_{SX}^6) \qquad [2b]$$

$$R_{CC} = \tfrac{1}{5}J(0)(\mu_0/4\pi)^2 h^2 \gamma_S^2 \gamma_I \gamma_X$$
$$\times (3\cos^2\alpha - 1)/(4\pi^2 r_{SI}^3 r_{SX}^3). \qquad [2c]$$

For $T \ll R_{CC}^{-1}$, it can then be shown that the effect of cross correlation changes the J value derived from the experiment of Fig. 1 by about $-2R_{CC}(T - \Delta)J_{XS}$ relative to the true one-bond J_{IS} value. Depending on the sign of the J coupling and the angle α, this cross-correlation contribution can be either positive or negative. Its magnitude can be a significant fraction of J_{XS}, and the cross-correlation effect therefore can alter the measured $^1J_{CH}$ value by up to several hertz. However, the transverse relaxation rate in proteins is dominated by $J(0)$ spectral-density terms, and the cross-correlation term is therefore nearly independent of the field strength. Therefore, to a good approximation, cross correlation does not interfere with extracting dipolar coupling constants from the J_{CH} values measured at different field strengths. It is also interesting to note that the above-mentioned cross-correlation effect interferes with virtually all types of J-coupling measurements, including measurement of $^1J_{CH}$ from the ^{13}C splitting in a 2D or 1D spectrum. For the latter case, if $R_{CC} > 0$ and $J_{IS} \times J_{XS} > 0$, the outer pair of multiplet components (corresponding to $|\alpha\alpha\rangle$ and $|\beta\beta\rangle$ spin states of I and X) are broader than the inner pair. If the J_{XS} splitting is unresolved in the S-spin spectrum, this then will result in a small reduction of the measured peak-to-peak splitting of the unresolved doublet relative to J_{SI} (Fig. 2B).
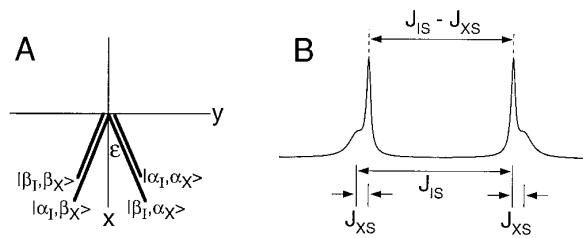

FIG. 2. Effects of evolution and relaxation on the S spin of an ISX spin system. (A) Magnetization vectors in the transverse plane after evolution for a period $2T = (N + \tfrac{1}{2})/J_{IS}$ and starting as pure antiphase magnetization $(2S_yI_z)$. The angle ϵ equals $2\pi TJ_{XS}$. Assuming $(3\cos^2\alpha - 1)\gamma_I\gamma_X > 0$, the S-spin multiplet components corresponding to $|\alpha_I, \alpha_X\rangle$ and $|\beta_I, \beta_X\rangle$ relax faster than the $|\alpha_I, \beta_X\rangle$ and $|\beta_I, \alpha_X\rangle$ multiplet components, resulting in a nonzero $2S_yI_z$ component. (B) S-spin multiplet shape with exaggerated effect of relaxation interference to show the distorted $^1J_{IS}$ splitting.
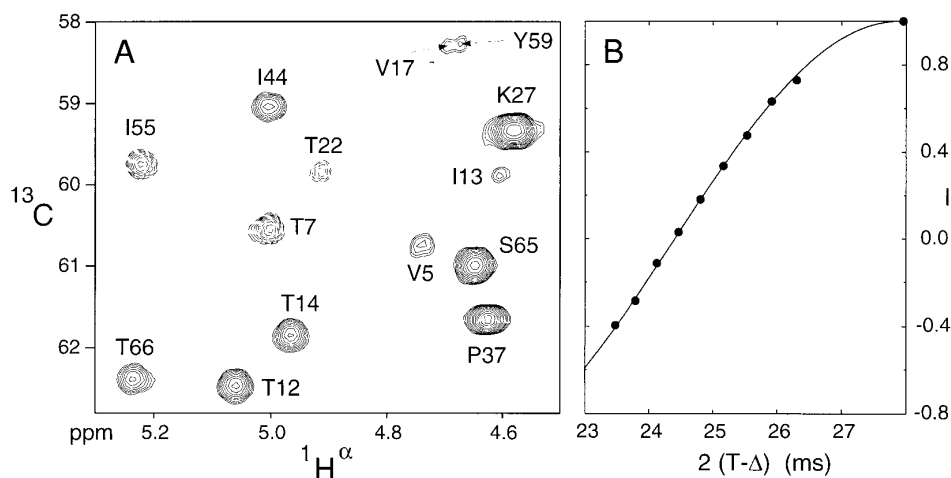
FIG. 3. (A) Small region of the 750 MHz 2D $^1J_{CH}$-modulated $^{13}C-^1H$ CT-HSQC spectrum of ubiquitin in H_2O, recorded for $\Delta = 1.6$ ms, and (B) intensity of the Thr^{14} $^1H^\alpha-^{13}C^\alpha$ correlation as a function of the dephasing delay, $2T - 2\Delta$, fit to $\cos[2\pi\, ^1J_{C\alpha H\alpha}\,(T - \Delta)]$. Dashed contours correspond to negative intensity.

Measurement of $^1J_{CH}$ is demonstrated for a sample of uniformly $^{15}N/^{13}C$-enriched human ubiquitin, 1.5 mM, pH 4.3, 95% H_2O, 5% D_2O, in a 230 μl Shigemi microcell. Spectra were recorded at 30°C on a Bruker AMX-360 spectrometer, equipped with a broadband inverse detection probehead, and on a DMX-750 spectrometer, equipped with a triple-resonance ($^1H/^{13}C/^{15}N$) probehead. Experiments at 360 MHz were carried out without ^{15}N decoupling. Both the 360 and 750 MHz probes contained self-shielded gradient coils.

Figure 3A shows a small region of the 750 MHz CT-HSQC spectrum, recorded with the pulse scheme of Fig. 1. As can be seen, the solvent suppression is excellent, and no additional noise at the H_2O F_2 frequency (4.73 ppm) can be detected, permitting accurate intensity measurement of the $^1H^\alpha-^{13}C^\alpha$ correlations. Figure 3B shows a fit between the experimental resonance intensities, obtained for the various durations of 2Δ, and the intensity modulation function, $C \times \cos[2\pi\, ^1J_{CH}\,(T - \Delta)]$. The experiment was carried out twice, yielding a pairwise root-mean-square deviation (rmsd) between the two sets of J couplings of 0.14 Hz, indicating a random error of only ±0.07 Hz in the averaged values. Duplicate measurements at 360 MHz were less reproducible and indicated a random error of 0.1 Hz in the averaged values. The $^1J_{CH}$ values, derived from measurements at the two fields, are shown in Fig. 4.

As shown in Fig. 5, the difference in $^1J_{CH}$ splitting at the two fields correlates with the dipolar contributions expected on the basis of the orientation of the $C^\alpha-H^\alpha$ bond vectors taken from the ubiquitin crystal structure (17) and its magnetic susceptibility tensor. The correlation coefficient, r, for this correlation equals 0.64, and the probability, p, that this correlation occurs by chance is negligible ($p < 10^{-6}$).

Accurate measurement of ^1J is considerably more difficult for $C^\alpha-H^\alpha$ pairs than for backbone N–H. However, as the

dipolar couplings are approximately twofold larger, this partially offsets the lower precision obtainable for $^1J_{CH}$. In practice, the combination of both N–H and $C^\alpha-H^\alpha$ dipolar coupling constraints in structure calculation is particularly powerful as together these couplings restrain the possible conformations of the polypeptide backbone considerably more than either type of coupling by itself. In this respect, it is also important to note that the value of $^1J_{C\alpha H\alpha}$ has also been related to the polypeptide backbone angles according to the relation (18)

$$^1J_{C\alpha H\alpha} = 138.8 + 1.74 \sin(\psi + 138°)$$
$$- 4.1 \cos 2(\psi + 138°) + 2.0 \cos 2(\phi + 30°). \quad [3]$$

The pairwise difference between the measured values and
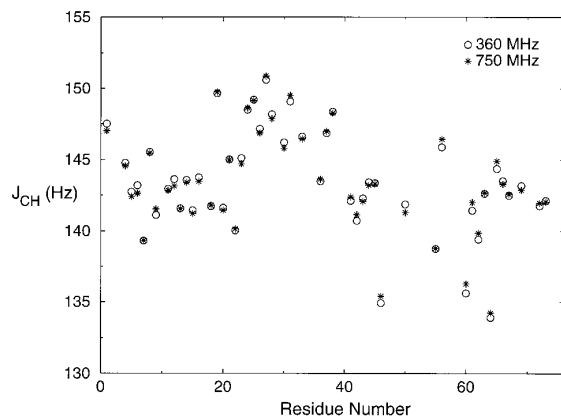

FIG. 4. Values of $^1J_{C\alpha H\alpha}$ as a function of residue number at 8.5 and 17.5 T (360 and 750 MHz ^1H frequency), as measured with the scheme of Fig. 1.
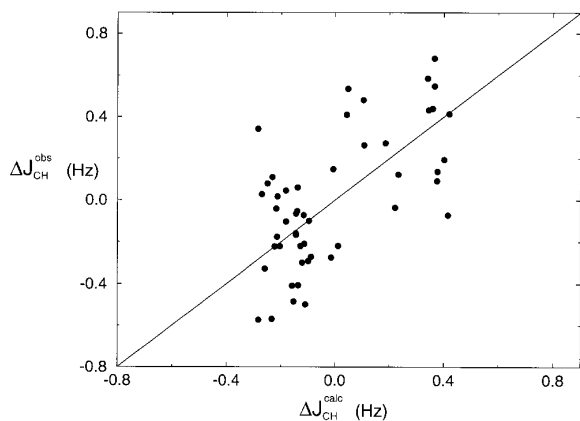
FIG. 5. Measured change in $^1J_{C\alpha H\alpha}$ (value at 750 MHz minus value at 360 MHz ^{1}H frequency) versus predicted difference in dipolar contribution, ΔJ_{CH}^{calc}, calculated using axial ($\Delta\chi_a$) and rhombic ($\Delta\chi_r$) components of the magnetic susceptibility anisotropy tensor derived from the dipolar contributions to backbone $^1J_{NH}$ splittings, measured at 750 and 360 MHz ($\Delta\chi_a = -2.35 \times 10^{-28}$ cm^3/molecule; $\Delta\chi_r = 0.46 \times 10^{-28}$ cm^3/molecule; $\theta = 51°$; $\phi = 118°$; $\psi = -71°$, where θ, ϕ, and ψ are the Euler angles describing the orientation of the susceptibility tensor in the X-ray coordinate frame). Note that the rhombic component based on the measurements at 750 and 360 MHz is smaller than the value previously found from measurements at 600 and 360 MHz, and now is closer to the values calculated from the sum of the contributions from peptide bonds and aromatic rings (9).

the predicted $^1J_{C\alpha H\alpha}$ values, using Eq. [3] and crystallographically determined ϕ and ψ angles, equals only 1.5 Hz. This is 0.5 Hz less than what was found when this empirical relation was initially derived. Note, however, that the constant factor of 138.8 in Eq. [3] is 1.5 Hz smaller than the value previously derived from measuring splittings in the ^{1}H dimension instead of the ^{13}C dimension. This difference is attributed to the different cross-correlation terms operative in the two types of experiments.

We have shown that residual dipolar ^{13}C–^{1}H dipolar contributions, resulting from incomplete rotational averaging, can be measured in a ^{13}C-enriched diamagnetic protein with a very small magnetic susceptibility anisotropy tensor. The RMS difference between the predicted and measured dipolar coupling equals 0.32 Hz, indicating that these dipolar couplings can be measured quite accurately. However, for ubiquitin, the magnitude of the dipolar ^{13}C$^\alpha$–^{1}H$^\alpha$ couplings relative to the uncertainty in their measurement is too low to permit their use in structure calculation of this protein. Much stronger magnetic alignment is found in paramagnetic proteins and in diamagnetic systems where aromatic groups are oriented roughly parallel to each other, such as found in double-helical nucleic acids. Proteins complexed with such DNA or RNA oligomers exhibit the same degree of magnetic alignment as the nucleic acid, resulting in dipolar couplings

which are much larger than the uncertainty in their measurement. In these cases, the dipolar couplings provide powerful constraints during protein structure calculation (19).

REFERENCES

1. C. Gayathri, A. A. Bothner-By, P. C. M. van Zijl, and C. MacLean, I, *Chem. Phys. Lett.* **87,** 192 (1982).

2. E. W. Bastiaan, C. MacLean, P. C. M. van Zijl, and A. A. Bothner-By, *Annu. Rep. NMR Spectrosc.* **19,** 35 (1987).

3. A. A. Bothner-By, C. Gayathri, P. C. M. van Zijl, C. Maclean, J.-J. Lai, and K. M. Smith, *Magn. Reson. Chem.* **23,** 935 (1985).

4. A. A. Bothner-By, *in* ''Encyclopedia of Nuclear Magnetic Resonance'' (D. M. Grant and R. K. Harris, Eds.), p. 2932, Wiley, Chichester, 1995.

5. C. R. Sanders, B. J. Hare, K. P. Howard, and J. H. Prestegard, *Prog. NMR Spectrosc.* **26,** 421 (1994).

6. B. A. Salvatore, R. Ghose, and J. H. Prestegard, *J. Am. Chem. Soc.* **118,** 4001 (1996).

7. J. R. Tolman, J. M. Flanagan, M. A. Kennedy, and J. H. Prestegard, *Proc. Natl. Acad. Sci. USA* **92,** 9279 (1995).

8. H. C. Kung, K. Y. Wang, I. Goljer, and P. H. Bolton, *J. Magn. Reson. B* **109,** 323 (1995).

9. N. Tjandra, S. Grzesiek, and A. Bax, *J. Am. Chem. Soc.* **118,** 6264 (1996).

10. J. Santoro and G. C. King, *J. Magn. Reson.* **97,** 202 (1992).

11. F. J. M. van de Ven and M. E. P. Philippens, *J. Magn. Reson.* **97,** 637 (1992).

12. G. W. Vuister and A. Bax, *J. Magn. Reson.* **98,** 428 (1992).

13. G. W. Vuister, F. Delaglio, and A. Bax, *J. Biomol. NMR* **3,** 67 (1993).

14. L. E. Kay, P. Keifer, and T. Saarinen, *J. Am. Chem. Soc.* **114,** 10,663 (1992).

15. J. R. Tolman and J. H. Prestegard, *J. Magn. Reson. B* **112,** 245 (1996).

16. L. G. Werbelow, *in* ''Encyclopedia of Nuclear Magnetic Resonance'' (D. M. Grant and R. K. Harris, Eds.), p. 4072, Wiley, Chichester, 1995.

17. S. Vijay-Kumar, C. E. Bugg, and W. J. Cook, *J. Mol. Biol.* **194,** 531 (1987).

18. G. W. Vuister, F. Delaglio, and A. Bax, *J. Am. Chem. Soc.* **114,** 9674 (1992).

19. N. Tjandra, J. G. Omichinski, A. M. Gronenborn, G. M. Clore, and A. Bax, submitted.

20. P. Bachmann, W. P. Aue, L. Müller, and R. R. Ernst, *J. Magn. Reson.* **28,** 29 (1977).

21. A. L. Davis, J. Keeler, E. D. Laue, and D. Moskau, *J. Magn. Reson.* **98,** 207 (1992).